



Editorial

Lorenzo Zaninetti *

Filaments of galaxies and Voronoi diagrams

Abstract: The intersections between a spherical shell and the faces of Voronoi's polyhedrons are numerically evaluated. The nodes of these intersections are the points that share the same distances from three nuclei. The nodes are assumed to be the places where we will find clusters of galaxies. The cosmological environment is given by the coupling between the number of galaxies as function of the redshift and the LCDM cosmology.

Keywords: galaxy groups, clusters, and superclusters; large scale structure of the Universe Cosmology

PACS: Galaxy groups, clusters, and superclusters + large scale structure of the Universe

1 Introduction

The first catalog of clusters of galaxies contained 2712 clusters Abell (1958). The updated version brought the number of rich clusters to 4073, each having at least 30 members Abell et al. (1989). The second catalog of galaxies contained 29418 galaxies and 9134 clusters and was organized in six books Zwicky et al. (1961, 1963, 1966a,b, 1965); Zwicky & Kowal (1968). The online version of the Zwicky catalog of galaxies contains 19369 galaxies Falco et al. (1999). Another line of research organized the observations of galaxies in slices; the first being the second CFA2 redshift Survey Huchra et al. (1999). Other catalogs made by slices or which can be organized in slices are: the 2dfGRS Norberg et al. (2002); the 6dF Galaxy Survey 6dFGS Jones et al. (2004)); and the SDSS DR12 with 208,478,448 galaxies Alam et al. (2015). All these slices present filaments of galaxies, which points toward a cellular structure for the 3D spatial distribution of galaxies. A model for the cellular structure of the local universe can be represented in Voronoi Diagrams Icke & van de Weygaert (1987); van de Weygaert & Icke (1989). In this model the galaxies can

*Corresponding author: Lorenzo Zaninetti , Physics Department, via P.Giuria 1,, I-10125 Turin,Italy

be inserted on the faces of irregular polyhedrons Zaninetti (1991a, 1995). Recently, the analysis of filaments of galaxies with the Cosmic Web Reconstruction (CWR) has made enormous progress Chen et al. (2015a,b, 2016, 2017).

The rest of this paper is structured as follows. Section 2 introduces the adopted cosmological framework. Section 3 models the intersection between a sphere and the network of the Voronoi's faces. Finally, Section 4 reports on the theoretical filaments and clusters of galaxies at low and high values of redshift.

2 Adopted Cosmology

This section introduces two catalogs of galaxies (the Λ CDM and the pseudo-Euclidean cosmology), the statistics of the cosmic voids and the standard luminosity function (LF) for galaxies.

2.1 The adopted catalogs

The 2MASS Redshift Survey (2MRS) has 44599 galaxies between $0 < z < 0.17$ and covers 91% of the sky, see Huchra et al. (2012). The redMaPPer catalog has 25000 clusters of galaxies between $0.08 < z < 0.55$ and covers 24.2% of the sky, see Rykoff et al. (2014).

2.2 Luminosity distance

We review the existing knowledge on the luminosity distance, $D_L(z; H_0, c, \Omega_M, \Omega_\Lambda)$, which in the Λ CDM cosmology can be expressed in terms of a Padé approximant. We should provide: the Hubble constant, H_0 , as expressed in $\text{km s}^{-1} \text{Mpc}^{-1}$; the velocity of light, c , as expressed in kms^{-1} ; and the three numbers Ω_M , Ω_K , and Ω_Λ , (see Zaninetti (2016a) for more details). A numerical analysis of the distance modulus for the Union 2.1 compilation, see Suzuki et al. (2012), gives $H_0 = 69.81 \text{km s}^{-1} \text{Mpc}^{-1}$, $\Omega_M = 0.239$ and $\Omega_\Lambda = 0.651$. We now apply the minimax rational approximation, which is characterized by two parameters p and q , and we find a simplified expression for the luminosity distance, $D_{L,2,1}$, when $p = 2$ and $q = 1$

$$D_{L,2,1} = \frac{-151.187045 + 4991.403961 z + 1643.868844 z^2}{0.9262689263 + 0.03596637742 z} \quad (1)$$

for $0 < z < 4$.

This equation can be inverted to give a "new" expression for the redshift as a function of the luminosity distance in Mpc

$$z = 1.09395 \times 10^{-5} D_{L,2,1} - 1.51818 + 6.08321 \times 10^{-15} \times \sqrt{3.23395 \times 10^{18} D_{L,2,1}^2 + 1.4329 \times 10^{25} D_{L,2,1} + 6.47706 \times 10^{28}} \quad (2)$$

for $0 < D_{L,2,1} < 43094$.

The most simple model for the distance, d , in the local universe is that of the pseudo-Euclidean cosmology:

$$d(z; c, H_0) = \frac{zc}{H_0} \quad , \quad (3)$$

where we used $H_0 = 67.93 \text{ km s}^{-1} \text{ Mpc}^{-1}$, see Zaninetti (2016b).

The differences between the two distances are the luminosity distance and the pseudo-Euclidean distance, which can be outlined in terms of a percentage difference: Δ . For example, for d ,

$$\Delta = \frac{|D_L(z) - d(z)|}{D_L(z)} \times 100 \quad . \quad (4)$$

Figure 1 reports the two distances. For $z \leq 0.2$, the percentage difference is lower than 10%.

Therefore the boundary between low and high z can be fixed at $z = 0.2$.

2.3 Cosmic voids

A *first* catalog of cosmic voids can be found in Pan et al. (2012), where the effective radius of the voids, R_{eff} , has been derived

$$R_{eff} = 18.23 h^{-1} \text{ Mpc} \quad \text{Pan et al. 2012} \quad . \quad (5)$$

The *second* catalog is that of radii up to redshift $0.12 h^{-1} \text{ Mpc}$ in (SDSS-DR7), see Varela et al. (2012),

$$R_{eff} = 11.85 h^{-1} \text{ Mpc} \quad \text{Varela et al. 2012} \quad . \quad (6)$$

The *third* catalog is that of the Baryon Oscillation Spectroscopic Survey, see Mao et al. (2017),

$$R_{eff} = 57.53 h^{-1} \text{ Mpc} \quad \text{Mao et al. 2017} \quad . \quad (7)$$

In the following, we will calibrate our code on the average value of the three previous values: $\overline{R_{eff}} = 29.2 h^{-1} \text{ Mpc}$.

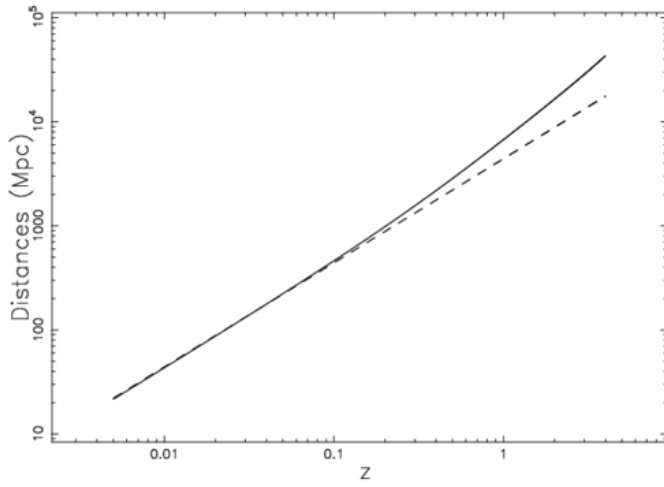


Fig. 1: The distances that are adopted are: the luminosity distance, D_L , in Λ CDM (full line); and the pseudo-Euclidean cosmology distance (dashed line).

2.4 The LF for galaxies

We now review the actual knowledge on the Schechter function, see Schechter (1976) which provides a useful standard for the LF of galaxies

$$\Phi(L)dL = \left(\frac{\Phi^*}{L^*}\right)\left(\frac{L}{L^*}\right)^\alpha \exp\left(-\frac{L}{L^*}\right)dL \quad , \quad (8)$$

where α sets the slope for low values of luminosity, L , L^* is the characteristic luminosity and Φ^* is the normalisation. The equivalent distribution in absolute magnitude is

$$\Phi(M)dM = 0.921\Phi^*10^{0.4(\alpha+1)(M^*-M)} \exp(-10^{0.4(M^*-M)})dM \quad , \quad (9)$$

where M^* is the characteristic magnitude as derived from the data. The scaling with h is $M^* - 5 \log_{10} h$ and $\Phi^* h^3$ [Mpc^{-3}]. According to formula (1.104) in Padmanabhan (1996) or formula (1.117) in Padmanabhan (2002) , the joint distribution in redshift, z , and flux, f , for galaxies in the pseudo-Euclidean cosmology, is

$$\frac{dN}{d\Omega dz df} = 4\pi \left(\frac{c}{H_0}\right)^5 z^4 \Phi\left(\frac{z^2}{z_{crit}^2}\right) \quad , \quad (10)$$

where $d\Omega$, dz and df represent the differential of the solid angle, the redshift and the flux, respectively, and Φ is the Schechter LF. The critical value of z , z_{crit} , is

$$z_{crit}^2 = \frac{H_0^2 L^*}{4\pi f c^2} \quad . \quad (11)$$

The number of galaxies in z and f as given by formula (10) has a maximum at $z = z_{pos-max}$, where

$$z_{pos-max} = z_{crit} \sqrt{\alpha + 2} \quad , \quad (12)$$

which can be re-expressed as

$$z_{pos-max}(f) = \frac{\sqrt{2 + \alpha} \sqrt{10^{0.4 M_\odot - 0.4 M^*} H_0}}{2 \sqrt{\pi} \sqrt{f} c} \quad , \quad (13)$$

where M_\odot is the reference magnitude of the sun at the considered bandpass. On replacing the flux f with the apparent magnitude m

$$z_{pos-max}(m) = \frac{1.772 \cdot 10^{-5} \sqrt{2 + \alpha} \sqrt{10^{0.4 M_\odot - 0.4 M^*} H_0}}{\sqrt{\pi} \sqrt{e^{0.921 M_\odot - 0.921 m} c}} \quad . \quad (14)$$

Figure 2 reports the number of observed galaxies of the 2MRS catalog for a given apparent magnitude and for the theoretical curve. Table 1 reports the parameters that were adopted in this model.

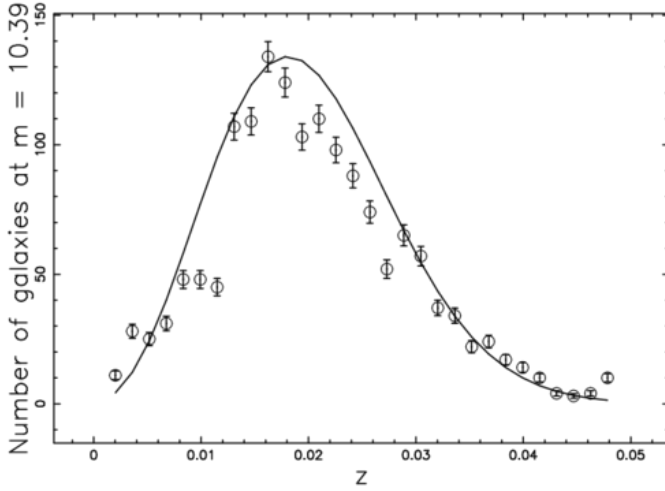


Fig. 2: The galaxies of the 2MRS with $10.31 \leq m \leq 10.47$ or $1164793 \frac{L_{\odot}}{Mpc^2} \leq f \leq 1346734 \frac{L_{\odot}}{Mpc^2}$ are organized in frequencies versus heliocentric redshift, (empty circles); and, the error bar is given by the square root of the frequency. The maximum frequency of observed galaxies is at $z = 0.017$. The full line is the theoretical curve generated by $\frac{dN}{d\Omega dz df}(z)$, see equation(10), and the maximum is at $z = 0.0133$. The parameters are given in Table 1.

Tab. 1: Parameters of the Schechter LF before scaling with h .

<i>parameter</i>	<i>value</i>
M^*	-23.15
α	-0.78
Φ^*	$0.0128/Mpc^3$
M_{\odot}	3.39
H_0	$67.93 \text{ km s}^{-1} \text{ Mpc}^{-1}$

The number of galaxies, $N(z, f_{min}, f_{max})$ comprised between a minimum value of flux, f_{min} , and maximum value of flux f_{max} , can be computed through the following integral

$$N(z) = \int_{f_{min}}^{f_{max}} 4\pi \left(\frac{c_l}{H_0}\right)^5 z^4 \Phi\left(\frac{z^2}{z_{crit}^2}\right) df \quad . \quad (15)$$

The indefinite integral exists in terms of the Whittaker function $M_{a,b}(x)$, see Abramowitz & Stegun (1965); Olver et al. (2010), but has a complicated expression. On inserting the model's parameters in this integral, we obtain the following "new" expression

$$N(z) = 9414469 z^2 \left(z^2\right)^{-0.39} e^{-249394.29 z^2} M_{-0.39, 0.11} \left(498788.58 z^2\right) - 106747137 z^2 \left(z^2\right)^{-0.39} e^{-493.043 z^2} M_{-0.39, 0.11} \left(986.0876 z^2\right) \quad . \quad (16)$$

The number of all of the galaxies for 2MRS as function of the redshift is visible in Figure 3. More details can be found in Zaninetti (2014).

3 Voronoi Diagrams

We now review the existing knowledge on the Voronoi diagrams. The faces of the Voronoi Polyhedra share the same property; i.e., they are equally distant from two nuclei or seeds. The intersection between a plane and the faces produces diagrams that are similar to the edges displacement in 2D Voronoi diagrams. From the point of view of the observations, it is very useful to study the intersection between a slice which crosses the center of the box and the faces of irregular polyhedrons where the galaxies presumably reside. According to the nomenclature reported in Okabe et al. (2000), this cut is classified as $V_P(2, 3)$. The parameters that will be used in the following are the kind of nuclei, which can be Poissonian or not Poissonian, the number of nuclei, the *side* of the box in *Mpc*, and the number of *pixels*, for example 1400, that are used to build the diagrams, see Zaninetti (1991b). The parameters adopted in the simulation of the pseudo-Euclidean cosmology are reported in Table2.

According to the nomenclature reported in Okabe et al. (2000), this cut is classified as $V_P(2, 3)$ and Figure 4 reports a typical example. This Figure also reports the spherical nodes that, in the absence of an official definition, can be defined as the locus of intersection between the lines of $V_P(2, 3)$. The spherical nodes are equally distant from three or four nuclei. The cross-sectional area of

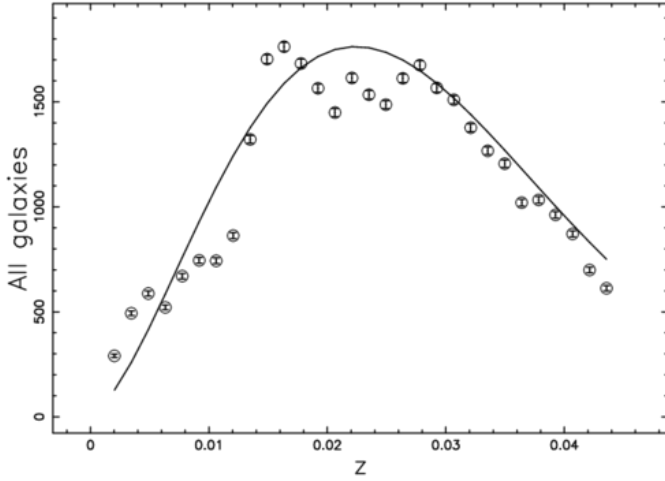


Fig. 3: All the galaxies for 2MRS are organised in frequencies versus redshift, (empty circles); the error bar is given by the square root of the frequency. The maximum frequency of the observed galaxies is at $z = 0.017$. The full line is the theoretical curve generated by the integral equation (16), which has maximum is at $z = 0.0237$. The parameters are given in Table 1.

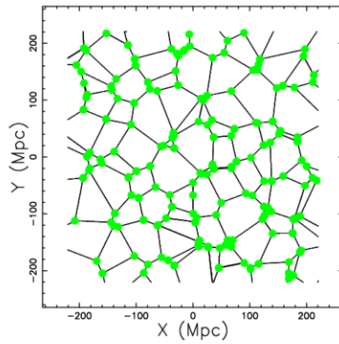
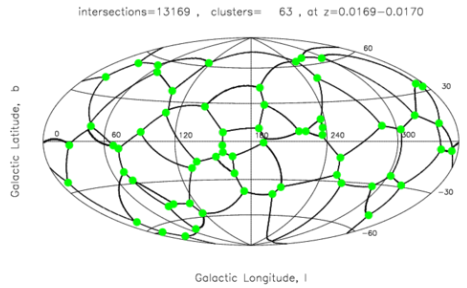


Fig. 4: Portion of the Poissonian Voronoi diagram $V_P(2,3)$; cut on the X-Y plane, black points, the parameters are given in Table 2. The spherical nodes are marked by great green points.

Tab. 2: Numerical values for the parameters of the Voronoi Diagrams.

catalog	Cosmology	pixels	type of seeds	seeds	box-side [Mpc]	radius [z]
2MRS	pseudo-Euclidean	1400	Poissonian	659	441	0.05
redMaPPer	Λ CDM	700	Poissonian	3914	1060	0.115


Fig. 5: The Voronoi-diagram $V_{P,s}(2,3)$ in the Hammer–Aitoff projection at $0.0169 < z < 0.0170$ with the same parameters as in Table 2.

the VP can also be visualised through a spherical cut that is characterised by a constant value of the distance to the center of the box, which in this case is expressed in z units. This intersection is not present in the Voronoi literature and therefore can be classified as a "new" topic. It may be called $V_{P,s}(2,3)$, where the index P, s stand for Poissonian and sphere respectively, see Figure 5. More details can be found in Zaninetti (2006).

4 Astrophysical Applications

This section reports the theoretical spatial display for clusters at low redshift, simulation of 2MRS, and at high redshift, simulation of redMaPPer.

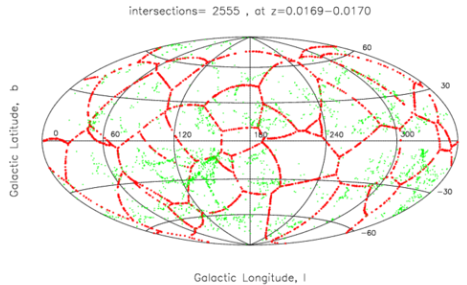


Fig. 6: The 2555 galaxies of 2MRS at $0.0169 < z < 0.0170$ (green points) and the same number of $V_{P,s}(2,3)$ in the Hammer–Aitoff projection (red points). The parameters are given in Table 2.

4.1 The 2MRS catalog

The photometric maximum in the number of galaxies as a function of z , see formula (16), has a maximum as a function of the redshift. Figure 6 reports an Hammer–Aitoff projection of the galaxies of 2MRS, as well the same number of $V_{P,s}(2,3)$. Figure 7 reports a cut of a given thickness, Δ , of 2MRS and a number of $V_P(2,3)$ chosen to scale as the number of galaxies.

4.2 The redMaPPer catalog

The number of clusters of the redMaPPer catalog as a function of the redshift has a maximum at $z \approx 0.346$, see Figure 8. Figure 9 reports the galaxies and clusters of the redMaPPer catalog. Figure 10 reports the same number of $V_{P,s}(2,3)$ and the spherical nodes with the same parameters as in Table 2.

5 Conclusions

Adopted Cosmology The local universe can be considered Euclidean up to $z \approx 0.2$, see Figure 1. At higher values of redshift, we need a luminosity distance

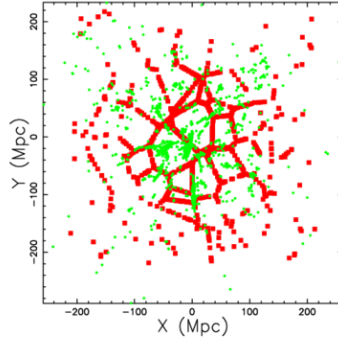


Fig. 7: A cut of the 3D spatial distribution of 2MRS in the $Z = 0$ plane when $\Delta = 4$ Mpc, the squared box has a side of 614 Mpc: we have 1384 galaxies (green filled circles). The same number of $V_P(2,3)$ (red squares) with radial scaling as the number of real galaxies with the same parameters as in Table 2.

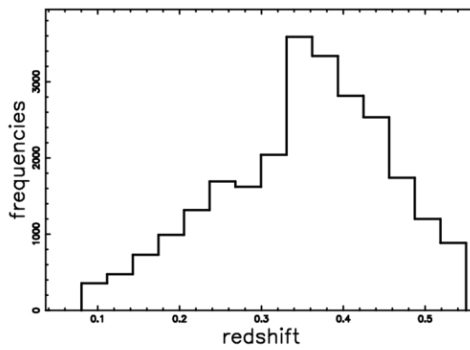


Fig. 8: Histogram (step-diagram) of the number of clusters in redMaPPer as a function of the redshift.

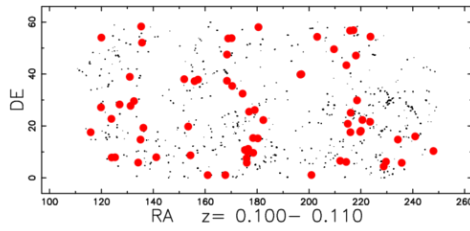


Fig. 9: Cut of the 3D spatial distribution of redMaPPer catalog at $0.1 < z < 0.11$: galaxies (black points) and clusters (red circles).

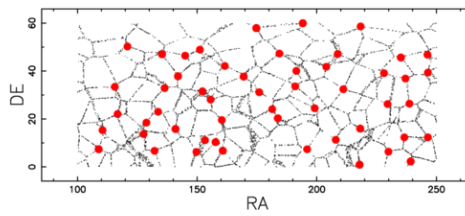


Fig. 10: $V_{P,s}(2,3)$ (black points) and spherical nodes (red circles) at $0.1 < z < 0.11$ or $480 \text{ Mpc} < D_{L484} < \text{Mpc}$. The numbers of galaxies and clusters are the same as in Figure 9.

versus redshift relationship in Λ CDM cosmology, see equation (2), and a redshift versus luminosity distance relationship, see equation (2).

Clusters of galaxies The geometrical nature for the clusters of galaxies is introduced in the framework of the intersection generated by a sphere with the faces of the Voronoi diagrams. At the same time, the exact number of galaxies and clusters as function of the redshift is regulated by photometric rules; i.e., a maximum in the number of galaxies, see Figure 2 for the 2MRS catalog. This maximum is also visible for the number of clusters as a function of the redshift, see Figure 8 for the redMaPPer catalog. A theoretical result for the spatial distribution of galaxies and clusters for the redMaPPer catalog is reported in Figure 10.

Acknowledgments

The 2MASS Redshift Survey is available at <http://cdsweb.u-strasbg.fr/>, the Vizier catalogue access tool, CDS, Strasbourg, France.

References

- Abell, G. O. 1958, *ApJS* , 3, 211
- Abell, G. O., Corwin, Jr., H. G., & Olowin, R. P. 1989, *ApJS* , 70, 1
- Abramowitz, M. & Stegun, I. A. 1965, *Handbook of Mathematical Functions with Formulas, Graphs, and Mathematical Tables* (New York: Dover)
- Alam, S., Albareti, F. D., Allende Prieto, C., & et al. 2015, *ApJS* , 219, 12
- Chen, Y.-C., Ho, S., Brinkmann, J., & et al. 2016, *MNRAS* , 461, 3896
- Chen, Y.-C., Ho, S., Freeman, P. E., & et al. 2015a, *MNRAS* , 454, 1140
- Chen, Y.-C., Ho, S., Mandelbaum, R. ., & et al. 2017, *MNRAS* , 466, 1880
- Chen, Y.-C., Ho, S., Tenneti, A., & et al. 2015b, *MNRAS* , 454, 3341
- Falco, E. E., Kurtz, M. J., Geller, M. J., et al. 1999, *PASP* , 111, 438
- Huchra, J. P., Macri, L. M., Masters, K. L., & et al. 2012, *ApJS* , 199, 26
- Huchra, J. P., Vogeley, M. S., & Geller, M. J. 1999, *ApJS* , 121, 287
- Icke, V. & van de Weygaert, R. 1987, *A&A* , 184, 16
- Jones, D. H., Saunders, W., Colless, M., Read, M. A., & Parker, Q. A. e. 2004, *MNRAS* , 355, 747
- Mao, Q., Berlind, A. A., Scherrer, R. J., & et al. 2017, *ApJ* , 835, 161
- Norberg, P., Baugh, C. M., Hawkins, E., Maddox, S., & Madgwick, D. e. a. 2002, *MNRAS* , 332, 827
- Okabe, A., Boots, B., Sugihara, K., & Chiu, S. 2000, *Spatial tessellations. Concepts and Applications of Voronoi diagrams*, 2nd ed. (Chichester, New York: Wiley)
- Olver, F. W. J. e., Lozier, D. W. e., Boisvert, R. F. e., & Clark, C. W. e. 2010, *NIST handbook of mathematical functions*. (Cambridge: Cambridge University Press.)



- Padmanabhan, P. 2002, *Theoretical astrophysics. Vol. III: Galaxies and Cosmology* (Cambridge, UK: Cambridge University Press)
- Padmanabhan, T. 1996, *Cosmology and Astrophysics through Problems* (Cambridge, UK: Cambridge University Press)
- Pan, D. C., Vogeley, M. S., Hoyle, F., Choi, Y.-Y., & Park, C. 2012, *MNRAS* , 421, 926
- Rykoff, E. S., Rozo, E., & et al. 2014, *ApJ* , 785, 104
- Schechter, P. 1976, *ApJ* , 203, 297
- Suzuki, N., Rubin, D., Lidman, C., et al. 2012, *ApJ* , 746, 85
- van de Weygaert, R. & Icke, V. 1989, *A&A* , 213, 1
- Varela, J., Betancort-Rijo, J., Trujillo, I., & Ricciardelli, E. 2012, *ApJ* , 744, 82
- Zaninetti, L. 1991a, *A&A* , 246, 291
- Zaninetti, L. 1991b, *A&A* , 246, 291
- Zaninetti, L. 1995, *A&AS* , 109, 71
- Zaninetti, L. 2006, *Chinese J. Astron. Astrophys.* , 6, 387
- Zaninetti, L. 2014, *Revista Mexicana de Astronomia y Astrofisica*, 50, 7
- Zaninetti, L. 2016a, *Galaxies*, 4, 4
- Zaninetti, L. 2016b, *Galaxies*, 4, 57
- Zwicky, F., Herzog, E., & Wild, P. 1963, *Catalogue of galaxies and of clusters of galaxies, Vol. II* (Pasadena: California Institute of Technology)
- Zwicky, F., Herzog, E., & Wild, P. 1966a, *Catalogue of galaxies and of clusters of galaxies, Vol. III* (Pasadena: California Institute of Technology)
- Zwicky, F., Herzog, E., & Wild, P. 1966b, *Catalogue of galaxies and of clusters of galaxies, Vol. IV* (Pasadena: California Institute of Technology)
- Zwicky, F., Herzog, E., Wild, P., Karpowicz, M., & Kowal, C. T. 1961, *Catalogue of galaxies and of clusters of galaxies, Vol. I* (Pasadena: California Institute of Technology)
- Zwicky, F., Karpowicz, M., & Kowal, C. T. 1965, "Catalogue of Galaxies and of Clusters of Galaxies", Vol. V (Pasadena: California Institute of Technology)
- Zwicky, F. & Kowal, C. T. 1968, "Catalogue of Galaxies and of Clusters of Galaxies", Volume VI (Pasadena: California Institute of Technology)